

# A PERFORMANCE ASSESSMENT OF POLARIMETRIC GNSS-R SEA LEVEL MONITORING IN THE PRESENCE OF SEA SURFACE ROUGHNESS

*M. Rajabi<sup>1</sup>, M. Hoseini<sup>1</sup>, H. Nahavandchi<sup>1</sup>, M. Semmling<sup>2</sup>, M. Ramatschi<sup>3</sup>,  
M. Goli<sup>4</sup>, R. Haas<sup>5</sup> and J. Wickert<sup>3,6</sup>*

<sup>1</sup> Norwegian University of Science and Technology NTNU, Trondheim, Norway

<sup>2</sup> Institute for Solar-Terrestrial Physics, German Aerospace Center (DLR-SO), Neustrelitz, Germany.

<sup>3</sup> German Research Centre for Geosciences GFZ, Potsdam, Germany

<sup>4</sup> Faculty of Civil & Architectural Engineering, Shahrood University of Technology, Iran

<sup>5</sup> Department of Space, Earth and Environment, Chalmers University of Technology, Gothenburg, Sweden

<sup>6</sup> Technische Universität Berlin, Berlin, Germany

## ABSTRACT

Monitoring coastal sea level has gained a large socio-economic and environmental significance. Ground-based Global Navigation Satellite System Reflectometry (GNSS-R) offers various geophysical parameters including sea surface height. We investigate a one-year dataset from January to December 2016 to evaluate the performance of GNSS-R coastal sea levels during different sea states. Our experiment setup uses three types of antenna in terms of polarization and orientation. A zenith-looking antenna tracks Right-Handed Circular Polarization (RHCP) signals and two sea-looking antennas capture both Left-Handed Circular Polarization (LHCP) and RHCP reflections. The Singular Spectrum Analysis (SSA) is used for extracting interferometric frequency from the data and calculating the heights. The results indicate that the height estimates from the sea-looking antennas have better accuracy compared to the zenith-looking orientation. The LHCP antenna delivers the best performance. The yearly Root Mean Square Errors (RMSE) of 5-min GNSS-R L1 water levels compared to the nearest tide gauge are 2.8 and 3.9 cm for the sea-looking antennas and 4.7 cm for the zenith-looking antenna with correlations of 97.63, 95.02, 95.35 percent, respectively. Our analysis shows that the roughness can both affect the GNSS-R retrieval accuracy and introduce a bias to the measurements.

**Index Terms**— Global Navigation Satellite Systems-Reflectometry (GNSS-R), Altimetry, Singular Spectrum Analysis (SSA)

## 1. INTRODUCTION

The characterization and accurate estimation of coastal waters can contribute to understanding the climate and environmental changes. This is also essential since a large population live in coastal areas and can be affected by associated natural disasters. Moreover, these areas are involved in substantial economic and trading activities. The

sea level also is a key parameter for defining vertical datum in geodesy.

Spaceborne Radar Altimeters (RA) and traditional Tide Gauges (TG) are the common instruments for sea-level monitoring. There are limitations associated with these techniques. The TG is pointwise and can be affected by vertical motions. The RA is restricted by its spatiotemporal resolution and lower performance over coastal areas [1, 2].

Besides positioning, navigation and timing, the Global Navigation Satellite System (GNSS) has been used for plenty of other applications. GNSS-Reflectometry as a novel remote sensing technique utilizes GNSS reflected signals from the earth surface to study various parameters and phenomena, e.g. sea-level and sea surface roughness [3], flood [5], sea-ice [6], soil moisture, ocean eddies [7], precipitation [8], wind speed, salinity, etc.

Ground-based GNSS-R for the sea-level altimetry has been used and the performance of the technique is proven. Most of the studies have used RHCP geodetic antennas and are limited to filter the data based on the elevation angles of signals. Therefore, investigation performance of the technique in different polarization and orientation of the antennas is desirable.

We aim to investigate the performance of the GNSS-R altimetry in three modes (3 types of antennas in different polarization and orientation) and the effect of the wind speed in the quality of the results. Three are various methods for spectral analysis such as least squares methods [9, 10] and Singular Spectrum Analysis (SSA). In this study, we apply the SSA which is a nonparametric and well-elaborated method for the times series analysis[11, 12], to estimate the interferometric frequency.

## 2. DATA AND METHODOLOGY

The data we used for proceeding in this study is the correlation sums at In-phase and Quadrature (I/Q) levels received by the GNSS Occultation, Reflectometry, and Scatterometry (GORS) receiver for each antenna. The

antennas installed at about 3 meters above the sea surface level and sea looking antennas have a 98° tilt with zenith. In addition, we utilize the other two ancillary data which one of them is the tide gauge observation placed 300 meters away from the GNSS-R station and another one is wind speed.

The methodology of this study is focused on estimating sea-level. We apply the period of interferometric oscillations to the I/Q time series to retrieve sea level as follow [14]:

$$\delta\rho = 2\delta H \sin(e), \delta f = \frac{2\delta H \cos(e)}{\lambda} \cdot \frac{de}{dt} \quad (1)$$

where  $\delta\rho$  is the Doppler shift,  $e$  is elevation angle of the traced signals,  $\delta H$  is the the height between antenna and sea surface and  $\delta f$  is the frequency which here we estimate using SSA. For detailed Information for SSA, readers could refer to [12, 13].

Overall, the current paper methodology contains three main steps, represented in Figure 1. The first step focuses on preparing received data from the receiver and eliminating the reflected data outside the sea. The second or main step concentrated on processing and started from making time-series for each PRN and reflection event and finished by outlier removal and finding the median of the sea surface height in the step of 5 min with the 3 hours' time window. The final step is to save the final estimated sea surface height and evaluate by the tide gauge observation in the different wind speed and consequently sea surface roughness.

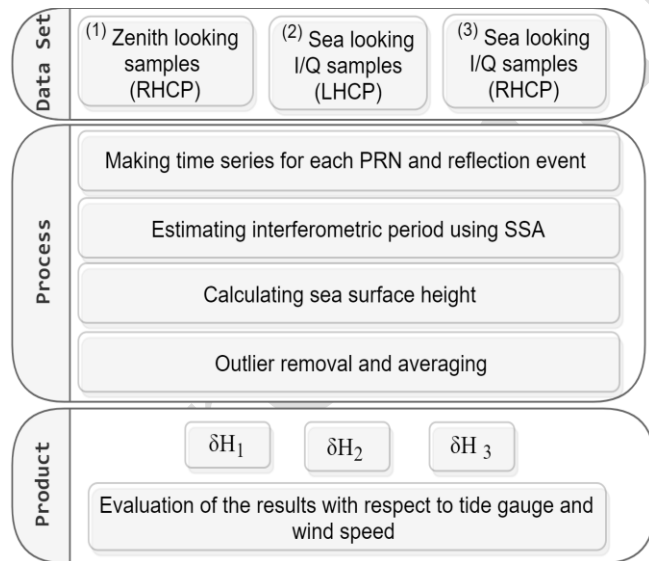


Fig. 1 Methodology flowchart based on the Singular Spectrum Analysis (SSA).

### 3. RESULTS AND DISCUSSION

The results of the SSA-based sea level retrievals from the GNSS-R dataset are presented and discussed in this section.

Figure 1 shows an exemplary case of applying SSA to I/Q time series to simultaneously extract the interferometric fringes as well as mitigating any unwanted components. As can be seen from the figure, the applied method can effectively reveal the changing amplitude of the interferometric signal. The detected peaks in the bottom panel of Fig. 1 is used to estimate the period of interest for calculation of height according to (1).

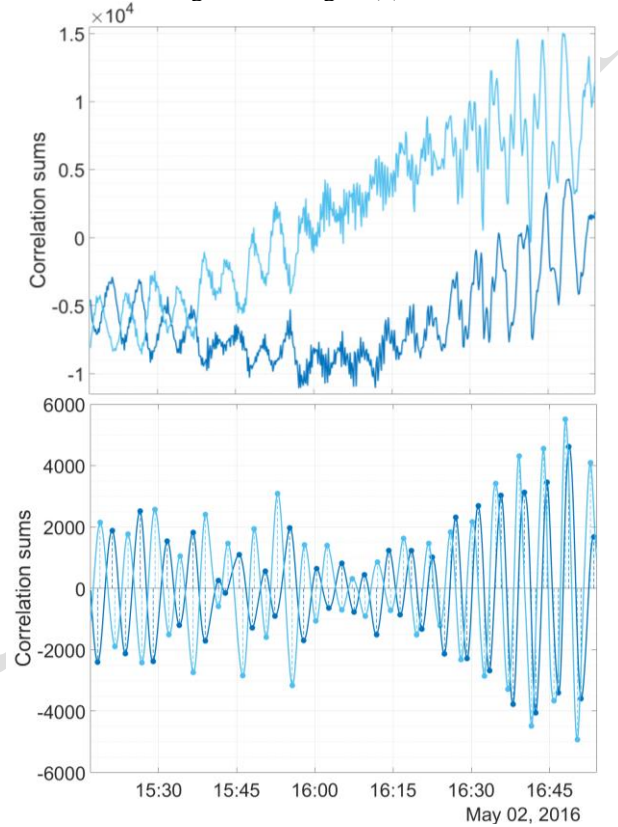


Fig. 1 - Top panel: an exemplary time series of in-phase / quadrature (I/Q) samples from GPS PRN 12 on May 02, 2016. Bottom panel: the retrievals of interferometric fringes from the I/Q correlation sums using Singular Spectrum Analysis (SSA). The dark and light blue are associated with in-phase and quadrature samples, respectively. The dots in the bottom panel show the detected I/Q peaks after applying SSA. The dashed lines are the amplitude estimates of I/Q components.

Figure 2 shows the joint distribution of sea level anomalies from GNSS-R and tide gauge. The measurements from the sea-looking LHCP antenna shown on the right panel show the best performance compared to both zenith-looking and sea-looking RHCP antennas. This can be perceived from the less dispersive and narrower joint distribution of the anomalies. The larger errors from the zenith-looking antenna in the left panel suggests that the change of the antenna orientation towards the sea can improve the GNSS-R sea level measurements.

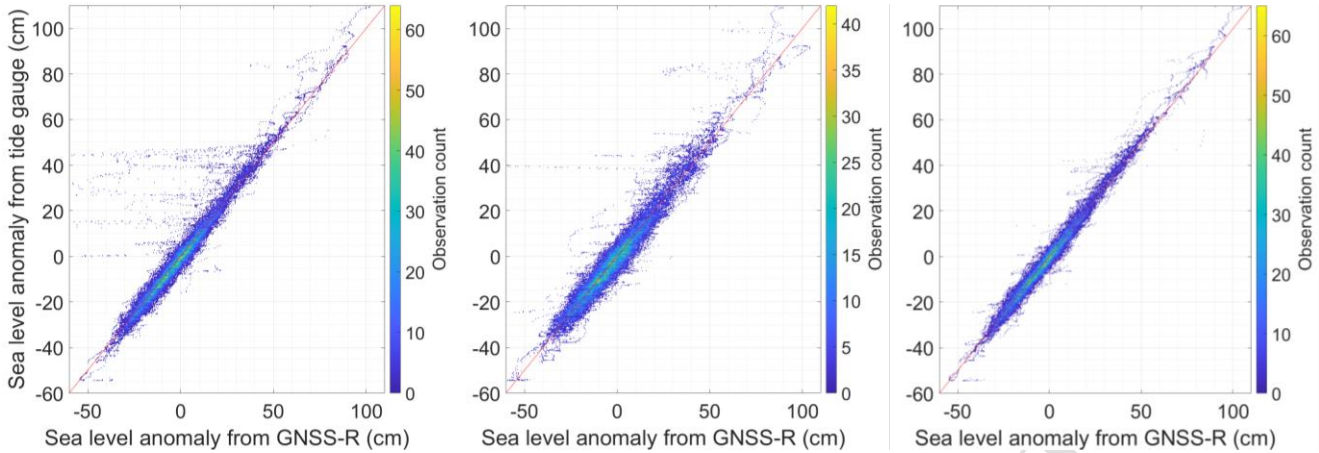


Fig. 2 – Comparisons of GNSS-R sea level measurements with respect to tide gauge data. The GNSS-R measurements are based on the application of Singular Spectrum Analysis (SSA) to the recorded observations from the antennas with different polarizations, i.e. Right and Left Handed Circular Polarization (RHCP and LHCP), and two orientations, i.e. zenith-looking and sea-looking. The left panel shows the results of the zenith-looking RHCP antenna, the middle panel is associated with the sea-looking RHCP antenna, and the right panel depicts the measurements from the sea-looking LHCP antenna. The red lines overlaid on the plots show the one to one relationship.

To evaluate the possible impact of sea surface roughness on the sea level measurement, we use the collocated wind measurements. Figure 3 gives an overview of the impact of different sea states on the accuracy of the measurements. The figure shows that for all of the antenna configurations increase of the wind speed degrades the accuracy of sea level retrievals. The investigation also reveals that the wind speeds can impose a bias in the measurements. The bias, in turn, has a notable contribution to the accuracy. Table 1 suggests that this contribution can adversely impact the overall yearly accuracy by about 1 cm.

It should be noted that the limited fetch of coastal GNSS-R experiments can partially shield the nearby sea surface

against some wind directions. As reported by [3], this can result in different sea surface roughness for wind speeds from different directions. The roughness estimates from the latter study based on the same dataset is used here to evaluate possible dependencies between the roughness and the GNSS-R sea level retrievals. The top panel in Fig. 4 provides an overview of roughness estimates against different wind speeds and directions. A delicate dependency of the height measurement errors and the roughness estimates can be seen in the bottom panel of Fig. 4.

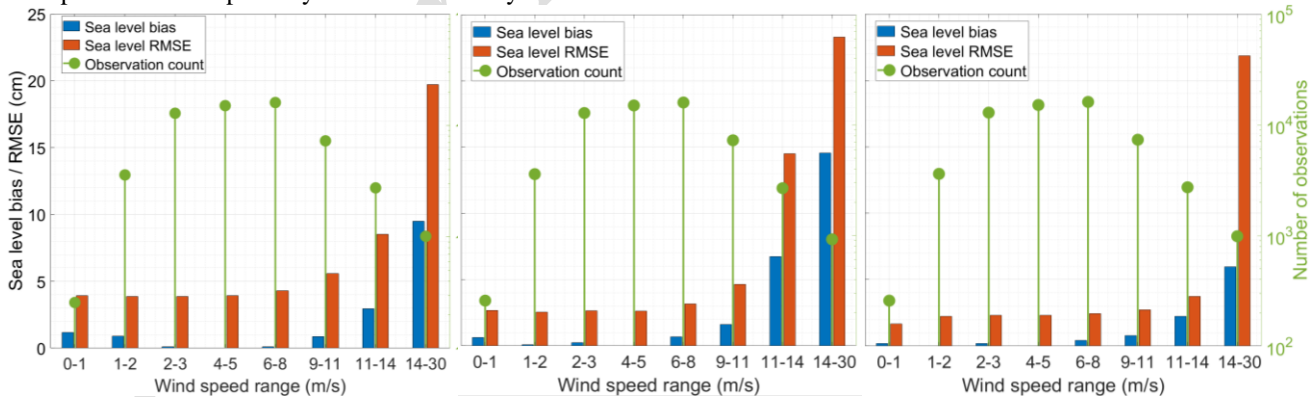


Fig. 3 - A performance assessment of GNSS-R sea level measurements at different ranges of wind speed. The sea level measurements are based on the application of Singular Spectrum Analysis (SSA) to the recorded observations from the antennas with different polarizations, i.e. Right and Left Handed Circular Polarization (RHCP and LHCP), and two orientations, i.e. zenith-looking and sea-looking. The left, middle, and right panels show the results from a zenith-looking RHCP antenna, a sea-looking RHCP antenna, and a sea-looking LHCP antenna, respectively. The blue bars are associated with the bias of the two datasets, i.e. the GNSS-R and tide gauge data, over each wind speed range. The red bars depict the Root Mean Squared Errors (RMSE) of the GNSS-R sea level measurements with respect to the tide gauge observations.

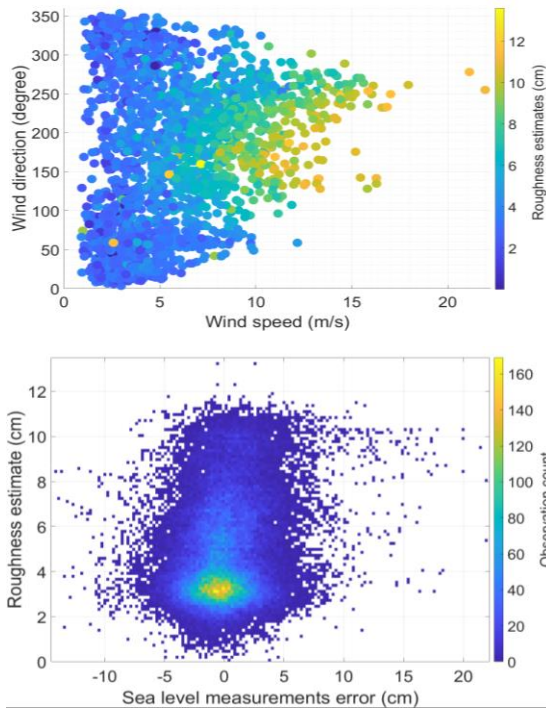


Fig. 4 - Top panel: estimates of sea surface roughness in terms of standard deviation of sea surface height based on different wind speed and direction. The estimates are obtained from [3]. Bottom panel: the distribution of GNSS-r sea level measurements error with respect to the sea surface roughness.

#### 4. CONCLUSION

The results of sea level measurements from GNSS-Reflectometry observations in a coastal experiment presented in this study. To retrieve these measurements, we applied Singular Spectrum Analysis (SSA) to the In-phase and Quadrature observations from three antennas with different polarizations and orientations. Comparison of collocated tide gauge observations with the GNSS-R sea level retrievals from different antenna polarizations and orientations reports an overall Root Mean Square Error (RMSE) ranging from 2.8 to 4.7 cm for a period of one year, i.e. from January to December 2016. The measurements from a seaward tilted Left-Handed Polarization (LHCP) antenna showed the best performance for sea level monitoring. The presence of measurement biases during different wind speeds were detected in the analysis. However, the reported biases could be higher for other GNSS-R experiments since the location of the setup in this study is surrounded by complex coastlines which can minimize the impact of winds. Our analysis shows that, even in this coastal configuration with suppressed wind effects, the overall RMSE can be degraded by about 1 cm if the roughness effect is not considered during the height retrievals.

#### 5. ACKNOWLEDGMENT

The authors would like to thank the Swedish Meteorological and Hydrological Institute (SMHI) and the Onsala Space Observatory (OSO), respectively, for the ancillary data and hosting the experiment.

#### 6. REFERENCES

- [1] F. Geremia-Nievinski *et al.*, "SNR-based GNSS reflectometry for coastal sea-level altimetry: results from the first IAG inter-comparison campaign," *Journal of Geodesy*, vol. 94, no. 8, pp. 1-15, 2020.
- [2] W. Liu *et al.*, "Coastal sea-level measurements based on gnss-r phase altimetry: A case study at the onsala space observatory, sweden," *IEEE Transactions on Geoscience and Remote Sensing*, vol. 55, no. 10, pp. 5625-5636, 2017.
- [3] M. Hoseini *et al.*, "On the Response of Polarimetric GNSS-Reflectometry to Sea Surface Roughness," *IEEE Transactions on Geoscience and Remote Sensing*, 2020.
- [4] M. Hoseini *et al.*, "On the Impact of Sea State on GNSS-R Polarimetric Observations," 2020.
- [5] M. Rajabi, H. Nahavandchi, and M. Hoseini, "Evaluation of CYGNSS Observations for Flood Detection and Mapping during Sistan and Baluchestan Torrential Rain in 2020," *Water*, vol. 12, no. 7, p. 2047, 2020.
- [6] A. M. Semmling *et al.*, "Sea-Ice Concentration Derived From GNSS Reflection Measurements in Fram Strait," *IEEE Transactions on Geoscience and Remote Sensing*, vol. 57, no. 12, pp. 10350-10361, 2019.
- [7] M. Hoseini, M. Asgarimehr, V. Zavorotny, H. Nahavandchi, C. Ruf, and J. Wickert, "First evidence of mesoscale ocean eddies signature in GNSS reflectometry measurements," *Remote Sensing*, vol. 12, no. 3, p. 542, 2020.
- [8] M. Asgarimehr, V. Zavorotny, J. Wickert, and S. Reich, "Can GNSS reflectometry detect precipitation over oceans?," *Geophysical Research Letters*, vol. 45, no. 22, pp. 12,585-12,592, 2018.
- [9] M. Rajabi, A. Amiri-Simkooei, J. Asgari, V. Nafisi, and S. Kiaei, "Analysis of TEC time series obtained from global ionospheric maps," *Journal of Geomatics Science and Technology*, vol. 4, no. 3, pp. 213-224, 2015.
- [10] M. Rajabi, A. Amiri-Simkooei, H. Nahavandchi, and V. Nafisi, "Modeling and Prediction of Regular Ionospheric Variations and Deterministic Anomalies," *Remote Sensing*, vol. 12, no. 6, p. 936, 2020.
- [11] S. Modiri, S. Belda, R. Heinkelmann, M. Hoseini, J. M. Ferrándiz, and H. Schuh, "Polar motion prediction using the combination of SSA and Copula-based analysis," *Earth, Planets and Space*, vol. 70, no. 1, p. 115, 2018.
- [12] M. Hoseini, F. Alshawaf, H. Nahavandchi, G. Dick, and J. Wickert, "Towards a zero-difference approach for homogenizing gnss tropospheric products," *GPS Solutions*, vol. 24, no. 1, p. 8, 2020.